行政院國家科學委員會專題研究計畫　成果報告

砷化鎵氮/砷化鎵 量子井在應變與鬆弛狀態下的電性研究

(3/3)

計畫類別：個別型計畫
計畫編號：NSC93-2112-M-009-002-
執行期間：93 年 08 月 01 日至 94 年 07 月 31 日
執行單位：國立交通大學電子物理學系(所)

計畫主持人：陳振芳

報告類型：完整報告

處理方式：本計畫可公開查詢

中　華　民　國 95 年 1 月 9 日

附件一

行政院國家科學委員會補助專題研究計畫 ☑成果報告 □期中進度報告

砷化鎵氮/砷化鎵 量子井在應變與鬆弛狀態下的電性研究

計畫類別：☑ 個別型計畫 □ 整合型計畫
計畫編號：NSC 93-2112-M-009-002-
執行期間： 93 年 08 月 01 日至 94 年 07 月 31 日

計畫主持人：陳振芳
共同主持人：
計畫參與人員：

成果報告類型(依經費核定清單規定繳交)：□精簡報告 ☑完整報告

本成果報告包括以下應繳交之附件：
□赴國外出差或研習心得報告一份
□赴大陸地區出差或研習心得報告一份
□出席國際學術會議心得報告及發表之論文各一份
□國際合作研究計畫國外研究報告書一份

處理方式：除產學合作研究計畫、提升產業技術及人才培育研究計畫、列管計畫及下列情形者外，得立即公開查詢
□涉及專利或其他智慧財產權，□一年□二年後可公開查詢

執行單位：國立交通大學

中 華 民 國 94 年 10 月 27 日

CONTENT

Contents……………………………………………………………………………2

Abstract (in English)……………………………………………………………..….3

Abstract (in Chinese)…………………………………………………………..….4

I. INTRODUCTION…………………………………………………………………5

II. RESEARCH PURPOSE……………………………………………………….5

III. RESEARCH METHODS……………………………………………………..5

IV. RESULTS and DISCUSSIONS…………………………………………….…….6

A. I-V characteristics of a thick $GaAs_{1-x}N_x$ (x=0.9%) layer

B. Deep-level transient spectroscopy (DLTS)

V. REFERENCES…………………………………………………………..……9

VI. FIGURES………………………………………………………………………10

VII. PUBLISHED PAPER…………………………………………………………13

VIII. SELF EVALUATION……………………………………………….……..…18

ABSTRACT

This proposal investigated the properties of (In)GaAsN/GaAs quantum wells in details. Thickness dependence of the properties of GaAsN grown on GaAs are investigated by characterizing GaAs/$GaAs_{0.982}N_{0.018}$/GaAs Schottky diodes by current-voltage (I-V), capacitance-voltage (C-V) profiling and deep-level transient spectroscopy (DLTS). I-V characteristics show a considerable increase in the saturation current when the GaAsN thickness is increased from 60 to 250 Å. As GaAsN thickness is increased further, the I-V characteristic deviates from that of a normal Schottky diode with a large series resistance.

Electrical conduction and defects in thick GaAsN grown on GaAs are also investigated. A 1.6-µm-thick $GaAs_{1-x}N_x$ (x=0.9%) layer grown on GaAs is found to be highly resistive, which is attributed to the presence of the E_1 (0.16 eV) and E_2 (0.74 eV) traps revealed by DLTS. The activation energy (capture cross-section) of the E_2 trap is found to be nearly independent of the N composition, suggesting that it is a GaAs intrinsic defect and, from its Arrhenius plots, it is likely an EL2 trap. This result suggests that the growth condition of GaAs incorporated by N atoms tends to be As-rich. Similar E_1 traps but with activation energies of 0.30 and 0.35 eV are observed in GaAs/GaAsN/GaAs heterostructures with N compositions of 1.2 and 1.8%, respectively. After comparing with optical emission energies, the increment of the activation energy is attributed to the conduction-band offset for GaAsN/GaAs. The E_1 trap is similar to a broad spectrum found in N-implanted GaAs in a dose of $2x10^{15}$ cm^{-2} after annealing at 500°C. Annealing at 700°C can remove this broad spectrum and simultaneously reduces the lattice expansion; thus, the formation of the E_1 trap is attributed to N-induced lattice expansion.

KEYWORDS: GaAsN/GaAs quantum wells, InAs self-assembled quantum dots, strain relaxation, carrier distribution and emission, deep traps, admittance spectroscopy, deep-level transient spectroscopy

中文摘要

我們藉由電流-電壓(I-V)、電容-電壓(C-V)，以及深層能階暫態頻譜分析儀(DLTS) 等量測，研究 GaAs/$GaAs_{0.982}N_{0.018}$/GaAs 蕭基二極體其 GaAsN 層對不同厚度的影響。從 I-V 特性上可看出，當 GaAsN 的厚度從 60Å 增加到 250Å 時，其飽和電流隨之明顯增加。若厚度繼續增加，其 I-V 特性將伴隨大串聯電阻的出現。

同時，我們也對厚 GaAsN 層成長在 GaAs 基板上其電傳導性及缺陷特性進行研究。在 GaAs 基板成長 1.6µm 厚的 $GaAs_{1-x}N_x$(x=0.9%)時，其電阻及劇增大的影響下，由 DLTS 可看到缺陷 E_1(0.16eV)和缺陷 E_2(0.74eV)的存在。我們發現缺陷 E_2 的活化能(捕獲截面積)幾乎和氮的濃度無關，推測其為 GaAs 的本質缺陷，且從 Arrhenius 圖得知此缺陷與 EL2 缺陷非常相像，由此結果可推知，在磊晶過程中隨著氮的加入，As 容易聚在一起。在氮含量為 1.2% 及 1.8% 的 GaAs/ GaAsN / GaAs 異質結構中，也找到相似的缺陷 E_1，只是活化能不同，分別為 0.30 及 0.35eV。比較其光性的激發能後，得知活化能增加是起因於 GaAsN / GaAs 傳導帶偏移量(offset)。用氮含量 $2x10^{15}$ cm^{-2} 離子佈植法所長的樣品，在 500˚C 熱退火後，其光譜很寬與缺陷 E_1 雷同。700˚C 熱退火可以消除此寬光譜且同時降低晶格膨脹；因此，缺陷 E_1 的形成歸因於氮引起的晶格膨脹。

I. INTRODUCTION

Recently, N-related compounds have attracted considerable attention due to their special physical properties and promising applications for long-wavelength optoelectronic devices.[1-7] However, obtaining good-quality GaAsN is difficult, probably due to a large miscibility gap.[8,9] GaAsN alloys grown at high temperatures are known to easily phase-separate.[10-12] It has been found that a post-growth annealing can improve the optical quality[13,14] and increase the diffusion length.[8] These studies imply that GaAsN layers grown on GaAs are enriched with defects. In addition, the lattice mismatch between GaN and GaAs may considerably degrade the quality of thick GaAsN layers.[12] In several publications, GaAsN/GaAs interfacial and deep defects[15,16] have been reported. In spite of this, very little is known about the detailed properties of the defects and the way they are influenced by N composition. It is our purpose in this work to characterize defect properties of GaAsN layers of different N compositions grown on GaAs.

II. RESEARCH PURPOSE

We have investigated the electrical defects in GaAsN layers grown on GaAs. Thick GaAsN layers grown on GaAs are resistive due to the presence of two traps, E_1 at 0.16 eV and E_2 at 0.74 eV. Two similar traps are observed in GaAs/GaAsN/GaAs samples. This result indicates that these two traps play a significant role in degrading the electrical quality of a thick GaAsN layer. The activation energies of these two traps are nearly independent of the N composition. After comparing these results with the defects in N-implanted GaAs after annealing, the formation of the E_1 trap is attributed to N-induced lattice expansion.

III. RESEARCH METHODS

Two sets of $GaAs_{1-x}N_x$ samples consisting of thick GaAsN and GaAs/GaAsN/GaAs heterojunction (HJ) samples were studied in this work. All samples were grown on n^+-GaAs (001) substrates by low-pressure metalorganic chemical vapor deposition. The thick GaAsN sample consists of a 0.5-μm-thick n-type GaAs buffer on top of which an undoped 1.6-μm-thick GaAsN layer was grown. In the HJ samples, an undoped GaAsN layer of different thickness and composition was inserted into a total 0.6-μm-thick Si-doped GaAs layer with a concentration of $6x10^{16}$ cm^{-3}. In both cases, the GaAsN layers were grown using dimethylhydrazine (DMHY) as a nitrogen source in combination with triethylgallium and AsH_3. The growth temperature was at 550°C. The N composition was determined by photoluminescence (PL) peaks and checked by double-crystal X-ray diffraction. Pendellosung interference fringes allow us to obtain accurately the GaAsN thickness. For a thin GaAsN layer that showed no Pendellosung interference fringes, the thickness was estimated from the growth time. Electrical properties of the HJ samples were measured on Au Schottky diodes with dot area of 0.0113 cm^2. Metal indium was used for an ohmic contact. Photoluminescence (PL) spectra were measured under the excitation of the 515-nm line from an Ar^+-ion laser. An HP4194A gain phase analyzer was used for characterizing capacitance-voltage (C-V) and capacitance-frequency (C-F) spectra.

IV. RESULTS and DISCUSSIONS

A. I-V characteristics of a thick $GaAs_{1-x}N_x$ (x=0.9%) layer

Thick $GaAs_{1-x}N_x$ layers grown on GaAs are found to be resistive. Figure 1(a) shows typical ohmic-contact current-voltage (I-V) characteristics for a 1.6-μm-thick GaAsN (x=0.9%) layer on GaAs. This sample, referred to as the "bulk" sample in the following, has a bandgap of 1.27 eV at 300 K from optical transmission measurement. As shown, the current consists of two distinct regions: a linear low-voltage region and an exponential high-voltage region. This current behavior is similar to that of an n-i-n structure whose low-voltage current is known to be mainly thermal activation of carriers. Therefore, the inverse of the slope in the linear region is taken as the resistance of the GaAsN layer, and the results are shown in Fig. 1(b) as a function of inverse temperatures. As shown, the 300 K resistance is as high as 6×10^5 Ω. At high temperatures (T>300 K), the temperature dependence of the resistance follows the thermally activated expression $R \propto T^{-3/2} \exp(E_{ac} / kT)$, where E_{ac} is the activation energy and k is the Boltzmann constant. This fitting gives E_{ac} = 0.38 eV, assuming a temperature-independent mobility, implying that the Fermi level in the GaAsN layer is at 0.38 eV below the conduction-band edge. Deep traps must exist to pin the Fermi level to such a deep depth. Figure 1(b) shows that at T<300K, the temperature dependence becomes weak. At T～140 K, the activation energy is only about 40 meV. This weak temperature dependence may be due to trap-assisted tunneling. This result implies that a thick GaAsN layer grown on GaAs is enriched with defects that deplete the carriers.

B. Deep-level transient spectroscopy (DLTS)

Figure 2 shows the DLTS spectra for the Schottky-contact bulk sample, along with two GaAs/GaAsN/GaAs HJ samples. For these measurements, the sweeping bias and rate windows are shown in the figure, with a filling pulse of 1 ms. As shown, the main features in the bulk sample are two dominant traps around 200 and 400 K, denoted as E_1 and E_2, respectively. These two traps were not detected in GaAs reference layers, and thus, they are induced by the N incorporation. The activation energies (capture cross-sections) of the E_1 and E_2 traps are determined to be 0.16 (2.58×10^{-19} cm^2) and 0.72 eV (3.65×10^{-15} cm^{-2}), respectively. Figure 3 shows that these traps are very weak. This cannot be interpreted as low densities, but can be accounted for by a difficulty of modulating the resistive GaAsN layer. The presence of these two traps can account for the high resistance in this sample. The fact that the Fermi level is pinned (at 0.38 eV) between these two traps suggests that both traps contribute to the high resistance.

Similarly, two traps are observed in the two HJ samples, as shown in Fig. 2. In these samples, the GaAsN thickness is kept at 250 Å, but the N compositions are 1.2 and 1.8%, respectively. The dc sweeping bias is chosen to include the GaAsN layer. The activation energies (capture cross-sections) of the E_1 trap are determined to be 0.30 (1.77×10^{-15} cm^2) and 0.35 eV (1.54×10^{-14} cm^{-2}) for the 1.2 and 1.8% samples, respectively. As for the E_2 trap, the activation

energies are 0.74 ($6.77x10^{-14}$ cm^2) and 0.75 eV ($5.38x10^{-14}$ cm^2) for the 1.2 and 1.8% samples, respectively. Note that in the 1.8% sample, the spectra show an additional weak trap around 300 K whose activation energy (capture cross-section) is determined to be 0.45 eV ($6.27x10^{-15}$ cm^2). The origin of this trap is unknown and is probably related to particular growth details; thus, it is not of interest to us. Figure 3 shows the Arrhenius plots of these traps. In the plots, we have included the data from C-F spectra measured on these two HJ samples. The C-F spectra are measured at a dc bias corresponding to the GaAsN layer. Because DLTS and C-F measurements probe very different temperature ranges, together they can yield rather accurate activation energy.

Let us consider the E_2 trap first. A similar trap was observed in InGaAsN.[16,17] Figure 4 shows that the activation energy (capture cross section) of the E_2 trap is nearly independent of the N composition. In terms of its energy position, this trap may give rise to the deep PL band observed by Buyanova *et al.*[18] at around 0.83 eV in GaAsN/GaAs multiple quantum wells. They found that the energy of the PL band is independent of N composition. This is consistent with our data. This composition independence suggests that the E_2 trap is pinned to the GaAs conduction band. The change in the surrounding atoms around this trap by different N content produces no appreciable effect on the properties of this trap. This result strongly suggests that the E_2 trap is a GaAs intrinsic defect. Judging from its Arrhenius plot, as shown in Fig. 3, it is likely an EL2 defect usually observed in GaAs. Because an As-rich growth condition is known for the formation of the EL2 trap, this result may suggest that the growth condition of the GaAsN layer tends to be As-rich due to the N incorporation.

As to the E_1 trap, we found that its activation energy increases from 0.16 to 0.30 and to 0.35 eV when the N composition is increased from 0.9 to 1.2 and to 1.8%, respectively. However, the different activation energies may be related to the different sample structure. For the 0.9 % bulk sample, it is certain that the activation energy represents the energy position of the trap relative to the GaAsN conduction band, whereas, for the 1.2 and 1.8% HJ samples, there exists a conduction-band offset ΔE_c for GaAsN/GaAs and the electrons need to overcome this energy barrier to emit from the GaAsN layer to the GaAs. Let us estimate the conduction-band offset from the PL spectra. Figure 4 shows the 10 K GaAsN-related peaks that are at 1.308 and 1.234 eV for 1.2% and 1.8% samples, respectively. These emission energies correspond approximately to the GaAsN bandgaps since the GaAsN layer (250 Å) is so thick that the quantum confinement is negligible. Although some controversy still remains over type-I or II band structure, the band offset for GaAsN/GaAs is known to be mainly in the conduction band. By using X-ray photoelectron spectroscopy, Kitatani *et al*[19]. obtained a change in the conduction (valence)-band offset with an increasing N content to be -0.175 eV/1%N (-0.019 eV/1%N). Our PL data yield a similar change of the conduction band offset of -0.123 eV/1%N. Using the relative ratio (~0.9) between ΔE_c and ΔE_v obtained by Kitatani *et al.,* and from a GaAs bandgap of 1.5 eV at 10 K, the PL data yield a conduction band offset of 0.173 and 0.239 eV for the 1.2 and 1.8 % samples, respectively. The increment of 0.066 eV is close to that of 0.05 eV in the activation energies of the E_1 trap with increasing the N composition from 1.2 to 1.8%, and thus, the increased activation energy can be attributed to the increased conduction-band offset. This result suggests that the trap is pinned to the GaAsN conduction-band edge and the electrons are emitted from the trap to the GaAs conduction band in the HJ samples. From the bulk sample, the trap lies at 0.16 eV below

the GaAsN conduction-band edge, after adding the conduction-band offset, the trap is at 0.333 (0.399) eV below the GaAs conduction-band edge which is close to the observed activation energy of 0.30 (0.35) eV of the E_1 trap in the 1.2 (1.8)% sample. This consistency leads us to believe that the E_1 trap is pinned at 0.16 eV below the GaAsN conduction-band edge and its energy position is independent of the N composition.

Properties of a defect are expected to alter due to changing the atoms surrounding it. Because the E_1 trap is induced by N incorporation, regardless its origin, the lineshape can be used to obtain information about the N composition fluctuation often observed in its related alloys. The N composition fluctuation will cause the fluctuation of atomic arrangements around the trap due to increased freedom of atomic arrangement, leading to a broadening of DLTS spectra as demonstrated by Yoshino *et al.*[20] for a defect in InGaAs(P). In both the HJ samples, the E_1 traps in Fig. 3 are rather sharp. In particular, no appreciable enhanced broadening is observed from 1.2 to 1.8%. This result suggests no appreciable N composition fluctuation. This is supported by their PL spectra in Fig. 4, which show no long low-energy tail. A GaAsN layer with N composition fluctuation would have locally various bandgaps, resulting in asymmetric PL spectra with a long-energy tail.[18] This result excludes the possibility that the E_1 trap originates from N composition disorder. The small linewidth (about 18 meV) of the PL peak also suggests that the samples are macroscopically uniform.

Due to considerable size difference between N and As atoms, increased incorporation of N atoms will substantially enhance local strain in the GaAsN layer. Let us examine whether the traps are related to strain relaxation. The X-ray diffraction patterns show no sign of strain relaxation for the HJ samples with the GaAsN layer (x=1.8%) up to 590 Å. Figure 5(a) shows the X-ray spectra along (004) diffraction for the HJ samples with different GaAsN thickness. In the case of 590 Å, the peaks at 33.03^{o} and 33.27^{o} are the GaAs and GaAsN peaks, respectively. The presence of Pendellosung fringes suggests flat GaAsN/GaAs interfaces, supporting a coherently strained GaAsN layer.[21] The coherent strain is supported by simulated spectra by dynamic theory. In the simulation, the Poisson ratios were taken to be 0.312 and 0.333 for GaAs and GaN, respectively, and the lattice constant of GaAsN was obtained from Vegard's law by using lattice constants of 5.653 and 4.526 Å for GaAs and GaN. As shown in Fig. 5(b), the experimental spectra of the 590-Å sample agree with the simulated spectra assuming coherent strain. This result indicates that these two traps are not induced by strain relaxation.

REFERENCES

[1]M. Kondow, S. Nakatsuka, T. Kitatani, Y. Yazawa, and M. Okai, Electron. Lett. **32**, 2244 (1996).
[2]S. Sato, Y. Osawa, and T. Saitoh, Jpn. J. Appl. Phys., Part 1 **36**, 2671 (1997).
[3]L. Bellaiche and A. Zunger, Phys. Rev. B **57**, 4425 (1998).
[4]S. R. Kurtz, A. A. Alleman, E. D. Jones, J. M. Gee, J. J. Banas, and B. E. Hammons, Appl. Phys. Lett. **74**, 729 (1999).
[5]S. Sakai, Y. Ueta, and Y. Teauchi, Jpn. J. Appl. Phys., Part 1 **32**, 4413 (1993).
[6]S. H. Wei and A. Zunger, Phys. Rev. Lett. **76**, 664 (1996).
[7]W. G. Bi and C. W. Tu, Appl. Phys. Lett. **70**, 1608 (1997).
[8]S. R. Kurtz, A. A. Alleman, E. D. Jones, J. M. Gee, J. J. Banas, and B. E. Hammons, Appl. Phys. Lett. **74**, 729 (1999).
[9]H. P. Xin and C. W. Tu, Appl. Phys. Lett. **72**, 2442 (1998).
[10]J. Neugerbauer and C. G. Van de Walle, Phys. Rev. B **51**, 10568 (1995).
[11]Y. Qiu, S. A. Nikishin, H. Temkin, V. A. Elyukin, and Yu. A. Kudriavtsev, Appl. Phys. Lett. **70**, 2831 (1997).
[12]Z. Pan, Y. T. Wang, L. H. Li, H. Wang, Z. Wei, Z. Q. Zhou, and Y. W. Lin, J. Appl. Phys. **86**, 5302 (1999).
[13]E. V. K. Rao, A. Ougazzaden, Y. Le Bellego, and M. Juhel, Appl. Phys. Lett. **72**, 1409 (1998).
[14]S. Francoeur, G. Sivaraman, Y. Qiu, S. Nikishin, and H. Temkin, Appl. Phys. Lett. **72**, 1857 (1998).
[15]P. Krispin, S. G. Spruytte, J. S. Harris, and K. H. Ploog, J. Appl. Phys. **88**, 4153 (2000).
[16]D. Kwon, R. J. Kaplar, S. A. Ringel, A. A. Alleman, S. R. Kurtz, and E. D. Jones, Appl. Phys. Lett. **74**, 2830 (1999).
[17]R. J. Kaplar, A. R. Arehart, S. A. Ringel, A. A. Allerman, R. M. Sieg, and S. R. Kurtz, J. Appl. Phys. **90**, 3405 (2001).
[18]I. A. Buyanova, W. M. Chen, G. Pozina, J. P. Bergman. H. P. Xin, and C. W. Tu, Appl. Phys. Lett. **75**, 501 (1999)
[19] T. Kitatani, M. Kondow, T. Kikawa, Y. Yazawa, M. Okai, and K. Uomi, Jap. J. Appl. Phys., Part 1 **38**, 5003 (1999).
[20]J. Yoshino, M. Tachikawa, N. Matsuda, M. Mizuta, and H. Kukimoto, Jap. J. Appl. Phys. **23**, L29 (1984).
[21]J. F. Chen, P. Y. Wang, J. S. Wang, N. C. Chen, X. J. Guo, and Y. F. Chen, J. App. Phys. **87**, 1251 (2000).

FIGURES

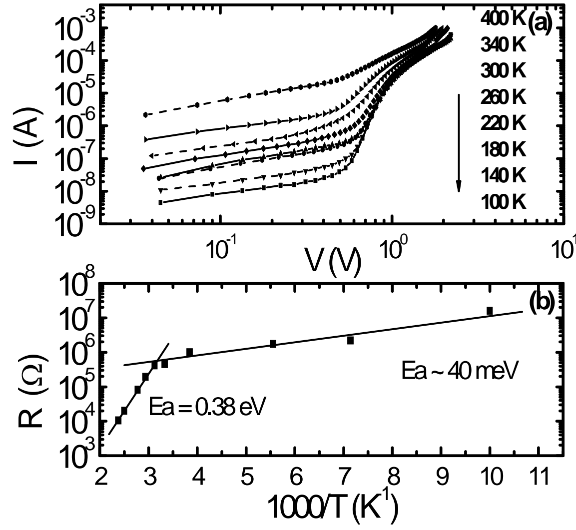

Fig. 1 (a) I-V characteristics of a 1.6-μm-thick $GaAs_{1-x}N_x$ (x=0.9%) layer grown on GaAs, exhibiting an Ohm's Law region at a voltage below 0.6 V with a room-temperature resistance of $6x10^5$ Ω. (b) The corresponding resistance as a function of reverse temperatures obtained from the Ohm's region.

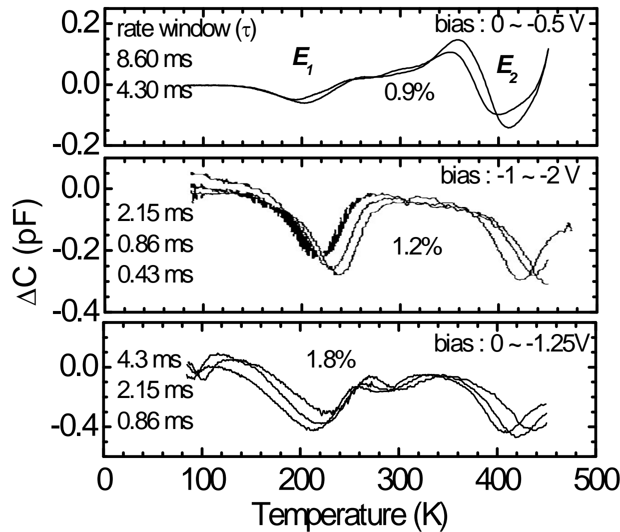

Fig. 2 DLTS spectra for the thick (x=0.9%) sample and two 250-Å $GaAs/GaAs_{1-x}N_x/GaAs$ HJ samples of x=1.2% and 1.8%. In each case, the main features of the spectra are two peaks around 200 and 400 K, denoted as E_1 and E_2, respectively.

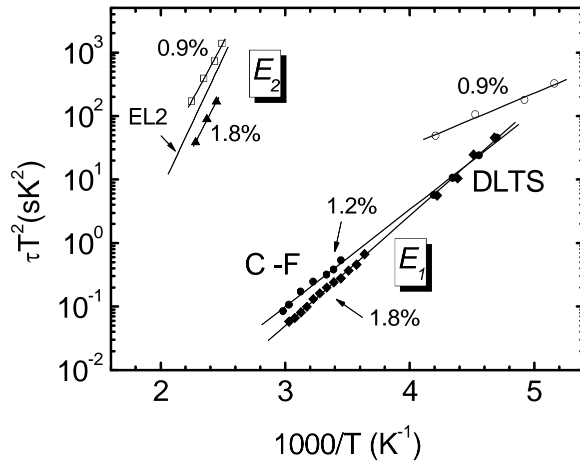

Fig. 3 Arrhenius plots of the E_1 and E_2 traps in Fig. 2, along with the time constants obtained from the C-F spectra for the two 250-Å HJ samples. Also included is an EL2 trap for comparison.

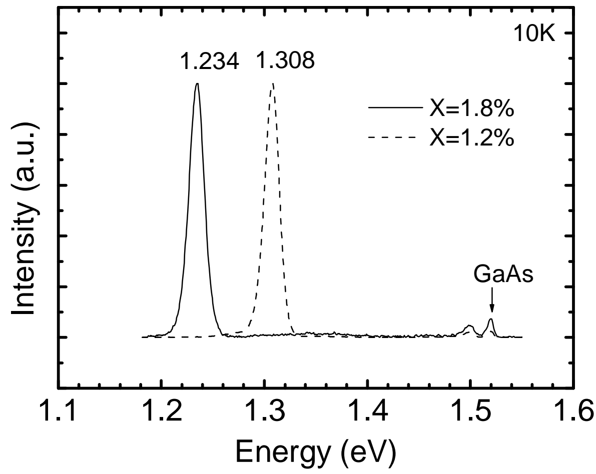

Fig. 4 10-K PL spectra for the two 250-Å HJ samples of x=1.2% and 1.8%. GaAsN-related peaks at 1.308 and 1.234 eV can be seen for the 1.2% and 1.8% samples, respectively.

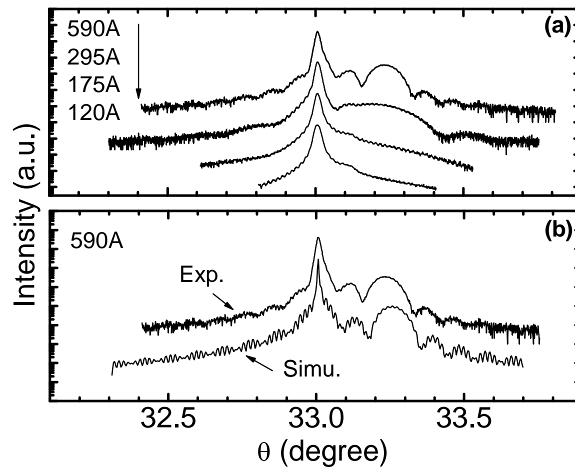

Fig. 5 (a) X-ray spectra along (004) diffraction for the $GaAs/GaAs_{0.982}N_{0.018}/GaAs$ HJ samples with different GaAsN thickness. The peaks at 33.03^{o} are the GaAs peaks. Pendellosung interference fringes can be seen in the 295 and 590-Å samples. (b) Comparison between the experimental and simulated spectra for the 590-Å sample assuming coherent strain.

The effect of thickness of the current conduction and carrier distribution of GaAsN on GaAs is also investigated and the results are published in Japanese Journal of Applied Physics, Vol. 44, No. 10, pp. 7507-7511, 2005. This paper is coped in the following:

Japanese Journal of Applied Physics
Vol. 44, No. 10, 2005, pp. 7507–7511

©2005 The Japan Society of Applied Physics

Thickness Dependence of Current Conduction and Carrier Distribution of GaAsN Grown on GaAs

Jenn-Fang CHEN, Ru-Shang HSIAO, Ming-Ta HSIEH, Wen-Di HUANG, P. S. GUO, Wei-I LEE, Shih-Chang LEE and Chi-Ling LEE

Department of Electrophysics, National Chiao Tung University, Hsinchu, Taiwan, R.O.C.

(Received February 3, 2005; revised June 9, 2005; accepted June 17, 2005; published October 11, 2005)

Thickness dependence of the properties of GaAsN grown on GaAs was investigated by characterizing GaAs/$GaAs_{0.982}N_{0.018}$/GaAs Schottky diodes by current–voltage (*I–V*), capacitance–voltage (*C–V*) profiling and deep-level transient spectroscopy (DLTS). *I–V* characteristics show a considerable increase in the saturation current when the GaAsN thickness is increased from 60 to 250 Å. As GaAsN thickness is increased further, the *I–V* characteristic deviates from that of a normal Schottky diode with a large series resistance. These *I–V* characteristics correlate well with carrier distribution. In thick GaAsN samples, *C–V* profiling shows carrier depletion in the top GaAs layer and frequency-dispersion accumulation in the GaAsN layer. DLTS spectra show that the carrier depletion in the top GaAs layer is due to an EL2 trap and the frequency-dispersion accumulation is due to the removal of electrons from a trap at 0.35 eV in the GaAsN layer. Increasing the GaAsN thickness markedly increases the magnitude of both traps. The large series resistance in thick GaAsN samples is due to EL2 that markedly depletes the top GaAs layer. [DOI: 10.1143/JJAP.44.7507]

KEYWORDS: GaAsN/GaAs, carrier distribution and emission, deep traps, deep-level transient spectroscopy

1. Introduction

GaAsN alloys have attracted considerable attention due to their unique physical properties and promising applications in long-wavelength optoelectronic devices.[1–4] A strong electron confinement induced by band gap reduction[5–7] upon N incorporation into GaAs has motivated research on this material. However, obtaining a high-quality GaAsN alloy is difficult due to N composition fluctuation,[8,9] phase separation,[10,11] low growth temperature and impurity incorporation. Layer quality deteriorates when GaAsN thickness or N content is increased.[9,12] It is well known that the optical quality of as-grown GaAsN alloys is poor but that it can be considerably improved by post growth annealing.[8,13,14] These studies imply that defects play a significant role in this material. However, very little is known about the properties of the defects[15,16] and their effects. Therefore, in this work, we investigated the thickness dependence of the properties of GaAsN layers grown on GaAs by current–voltage (*I–V*), capacitance–voltage (*C–V*) profiling, and deep-level transient spectroscopy (DLTS). Carrier distribution and defect traps were analyzed at different GaAsN thicknesses. Two defect traps at 0.35 and 0.75 eV were found to govern carrier distribution. Strain and optical properties were characterized by double-crystal X-ray diffraction (DC-XRD) and photoluminescence (PL) for comparison.

2. Experimental

GaAs/$GaAs_{0.982}N_{0.018}$/GaAs samples were grown on n^+-GaAs(001) substrates by low-pressure metalorganic chemical vapor deposition (LP-MOCVD). The top GaAs layer was grown in order to move the depletion-region edge across the GaAsN layer by the application of reverse voltage. Dimethylhydrazine (DMHY) was used as a nitrogen source in combination with triethylgallium and AsH_3 for growing the GaAsN layers. The GaAsN layer, about 0.3 µm from the surface, was sandwiched between two Si-doped GaAs layers with a concentration of $\sim 6 \times 10^{16}\,cm^{-3}$. The whole structure was grown at 550°C. The N composition is determined from the PL peak and confirmed by DC-XRD. Pendellosung interference fringes observed for 295- and 590-Å samples determined GaAsN thickness. Thickness thinner than 295 Å was estimated from the growth time. For electrical characterizations, the samples were fabricated as Schottky diodes by evaporating Au with a dot diameter of 1500 µm. A HP4194 gain phase analyzer was used for characterizing *C–V* and capacitance–frequency (*C–F*) spectra.

3. Measurement and Results

3.1 *I–V characterization*

Figure 1(a) shows the effect of GaAsN thickness on 300-K forward-bias *I–V* characteristics for the GaAsN thicknesses of 60, 250, 295, and 590 Å. Except for the 590-Å sample, reasonably good rectified curves with ideal factors in the range from 1.06 to 1.4 were obtained. Let us compare

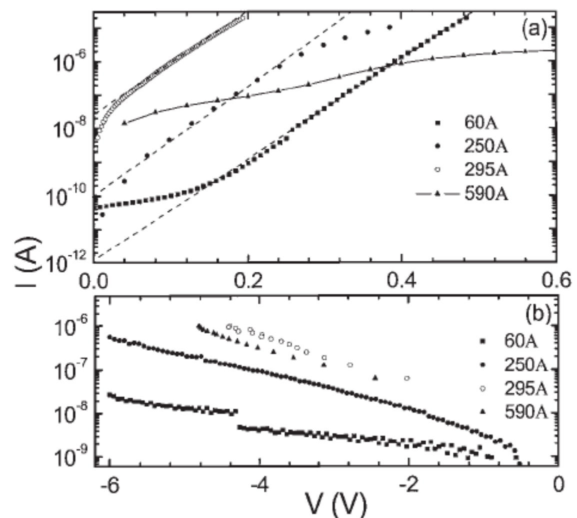

Fig. 1. (a) Forward-bias *I–V* curves at 300 K for GaAsN/GaAs Schottky diodes with different GaAsN thicknesses. The data show a degradation as the GaAsN thickness is increased. (b) Corresponding reverse-bias *I–V* characteristics at 300 K. The leakage current can be observed to increase with increasing GaAsN thickness from 60 to 295 Å.

their saturation current by extrapolating current to zero voltage. An increase in the saturation current from 10^{-12} to 10^{-10} and to 3×10^{-8} A can be observed as the GaAsN thickness is increased from 60 to 250 Å and to 295 Å, indicating a considerably degraded GaAsN layer. Leakage current can result from generation recombination, field emission or tunneling. Field emission or tunneling can take place if the depletion width is sufficiently small. As will be shown later, as GaAsN thickness is increased, the GaAsN layer becomes enriched with defects that cause carrier depletion. Thus, we exclude the possibility of field emission or tunneling, considering only the generation recombination current for the leakage current. Figure 1(a) shows a gradual increase in defect densities as GaAsN thickness is increased. Defects in the top GaAs layer also contribute a considerably part to the leakage current. When the GaAsN thickness is increased to 250-Å, carrier depletion was found to extend to the top GaAs layer, suggesting the presence of deep defects in the top GaAs layer. Figure 1(a) shows that the *I–V* curve of the 590-Å sample deviates from that of a normal Schottky diode. The pronounced broad shoulder at voltages lower than 0.3 V reflects the effect of significant defects. The current bending at large voltages in this sample indicates the presence of a large series resistance, which is attributed to a drastic carrier depletion in the top GaAs layer.

Figure 1(b) shows the corresponding reverse-bias *I–V* characteristics at 300 K. Leakage current can be observed to increase with increasing GaAsN thickness from 60 to 295 Å. For example, the leakage current at −4 V increased from 4×10^{-9} A for 60 Å, to 10^{-7} A for 250 Å, and to 8×10^{-7} A for 295 Å. This trend is consistent with that of saturation current found in forward-bias *I–V* characteristics. However, when the GaAsN thickness was further increased to 590 Å, the leakage current slightly decreased to 4×10^{-7} A. This reduction in current can be explained by the suppression of the large series resistance observed in the forward-bias current of this sample. It is interesting to note that the 60 Å sample displays an abrupt current jump at −4.4 V. A similar current jump was observed in a sample with a 40-Å-thick GaAsN layer. By comparison with their *C–V* curves, the voltages at which current jumps correspond to the location of the GaAsN layers. Significant amounts of carriers are confined in the GaAsN layer; and thus, it is conjectured that the current jump is due to the confined carriers that are swept out of the GaAsN region when dc voltage shifts the Fermi level well below the energy level of the GaAsN layer.

3.2 *C–V profiling*

Detailed apparent-concentration profiles are shown in Fig. 2 for 60-, 250- and 295- and 590-Å samples converted from *C–V* spectra with the voltage sweep from 0 to −6 V for the 60-Å sample and 0 to −3 V for the other three samples. The distribution of the depleted layer can be understood from this figure. In the 60-Å sample, the carrier accumulation peak is visible in the GaAsN region. An increase in magnitude is observed with decreasing temperature, which is characteristic of a Debye-length effect in a quantum-well structure. No suppression in the magnitude can be observed up to 1 MHz at 80 K, indicating a very rapid electron emission from the GaAsN quantum state, the presence of which is also indicated in PL spectra at 10 K that show a

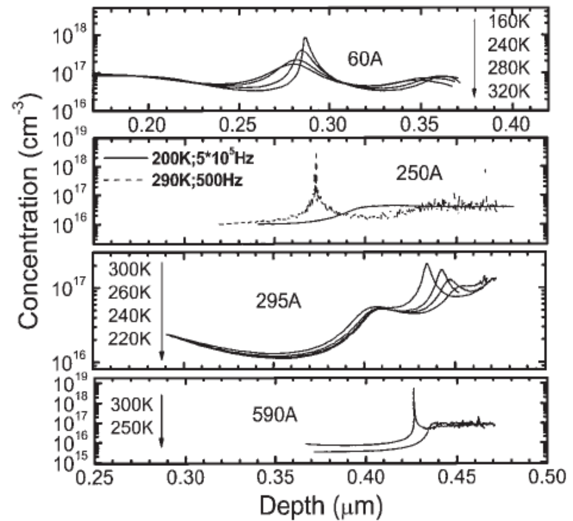

Fig. 2. Concentration profiles for 60-, 250-, 295- and 590-Å GaAsN/GaAs samples. A frequency-independent accumulation peak in the GaAsN region is observed for the 60-Å sample. Carrier depletion in the top GaAs layer and a frequency-dispersion accumulation peak in the GaAsN region are observed in 250-, 295- and 590-Å samples. The depletion in the top GaAs layer is increased as GaAsN thickness is increased.

GaAsN-related peak at 1.308 eV. However, when the GaAsN thickness is increased to 250 Å, the concentration profiles are not symmetric with a lower background concentration in the top GaAs layer, indicating carrier depletion in the top GaAs layer. In the next section, DLTS spectra show the presence of a deep trap at 0.75 eV in the top GaAs layer. An accumulation peak (0.37 μm) appears for the GaAsN layer at a low frequency and a high temperature as shown in Fig. 2, illustrating the presence of the peak at 290 K and 500 Hz; which is absent at 200 K and 5×10^5 Hz. This long emission time is characteristic of defect traps and the peak corresponds to the emptying of electrons from the traps. The narrowness of this peak suggests the confinement of the traps in the GaAsN layer or at the interface. Emission time can be obtained from the *C–F* spectra shown in Fig. 3, in which capacitance dispersion over frequency can be noted. The additional capacitance in the low-frequency limit arises from electron emission from the traps. The emission times, taken from the inverse inflection frequency at which capacitance drops from high to low plateaus, are shown in the Arrhenius plots as solid squares (indicated by admittance) in Fig. 4. The activation energy (capture cross section) was determined to be 0.34 eV (1.24×10^{-14} cm^2). These results show that as GaAsN thickness is increased, defect traps at 0.75 and 0.34 eV are formed in the top GaAs and GaAsN layers, respectively. When the GaAsN thickness is further increased to 295 and 590 Å, the depletion in the top GaAs layer becomes even worse and no peaks can be observed in the GaAsN layer even at a very low available frequency. Instead, a peak appears at approximately 0.43 – 0.45 μm, which is in the bottom GaAs layer. This peak cannot be explained by electron accumulation at that depth. It is believed to originate from the expulsion of trapped electrons from deep traps as dc voltage shifts the Fermi level to well below the trap levels. In the 590-Å sample, the

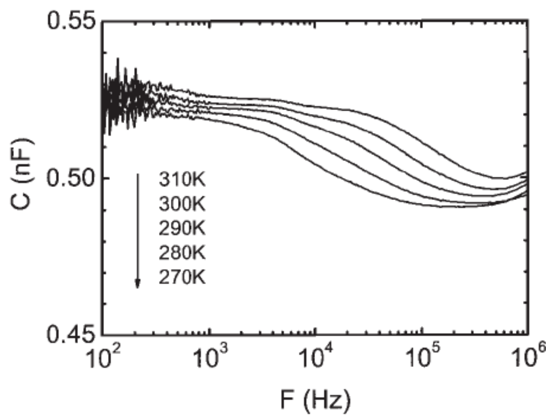

Fig. 3. *C–F* spectra of 250-Å sample at bias of −0.8 V corresponding to GaAsN layer. Capacitance dispersion indicates the presence of a trap at 0.35 eV in the GaAsN layer. This capacitance dispersion is due to the E_a trap shown in Fig. 5.

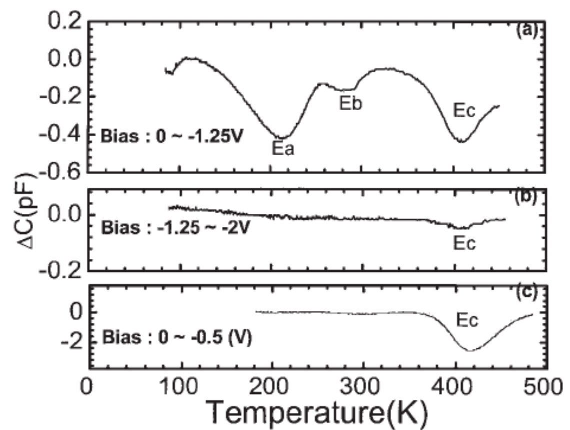

Fig. 5. DLTS spectra of 250-Å sample for (a) region including top GaAs and GaAsN layers, (b) and bottom GaAs and (c) top GaAs layers. These figures show that the E_a and E_b traps are in the GaAsN layer and the E_c trap is predominantly in the top GaAs layer.

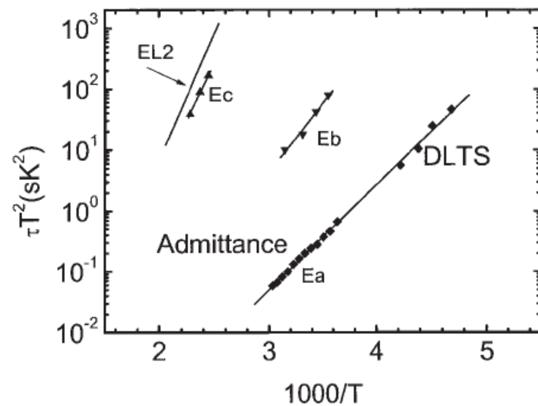

Fig. 4. Arrhenius plots from time constants observed in *C–F* and DLTS spectra. The solid squares indicating admittance are obtained from the *C–F* spectra shown in Fig. 3. Other data labeled E_a, E_b and E_c are obtained from the DLTS spectra of the 250-Å sample shown in Fig. 5. The data for EL2 are included for comparison.

background concentration in the top GaAs layer shows a considerable temperature dependence due to a strong impact of deep traps. This marked carrier depletion correlates well with deviated *I–V* characteristics with a very large series resistance. This result indicates that the top GaAs layer is markedly degraded after the growth of a thick GaAsN layer while the bottom GaAs layer is not much affected, as evident from its normal background concentration.

3.3 DLTS spectra

To identify the traps, DLTS spectra of each sample were measured. No DLTS signals were detected in the 40-Å sample. A very weak signal at approximately 200 K was detected in the 60-Å sample. However, this signal was too weak to obtain its activation energy. However, three traps in the 250-Å sample, labeled E_a, E_b and E_c are clearly visible in Fig. 5(a) for a region including the top GaAs and GaAsN layers. By changing sweeping bias, we can determine their spatial locations. Figures 5(b) and 5(c) show the spectra for the bottom GaAs and the top GaAs layers, respectively. As shown in this figure, the bottom GaAs layer is nearly free of traps (except very weak E_c). In contrast, the top GaAs layer is enriched with E_c trap. Note that the concentration of E_c is very high in the top GaAs layer. This result indicates that the E_a and E_b traps are in the GaAsN region but the E_c trap is mainly in the top GaAs layer. This trap distribution correlates well with carrier depletion, allowing us to identify that the E_c trap depletes the top GaAs layer. The Arrhenius plots for these traps are shown in Fig. 4. These plots show that the E_a trap gives rise to electron emission from the GaAsN layer observed in the *C–F* spectra shown in Fig. 3, as evidenced by a straight line connecting both the time constants together. Since the DLTS and *C–F* measurements (admittance) probe rather different temperature ranges, the activation energy (capture cross section) of the E_a trap can be obtained accurately to be 0.35 eV ($1.54 \times 10^{-14}\,cm^{-2}$). This trap depletes electrons in the GaAsN layer. As for the other two traps E_b and E_c, their activation energies (capture cross sections) were determined to be 0.45 ($6.27 \times 10^{-15}\,cm^2$) and 0.75 eV ($5.38 \times 10^{-14}\,cm^2$), respectively. Therefore, it is the trap at 0.75 eV that depletes the top GaAs layer. This can be further confirmed by the DLTS spectra of the 295-Å sample for the top GaAs layer as shown in Fig. 6. A dominant trap at about 400 K can be observed, which was identified to be the trap at 0.75 eV. A detail inspection of the spectra reveals a very weak signal at about 200 K (shown in the inset), whose intensity is too small to obtain a reliable activation energy; but determining on the basis of temperature, it is likely to be the 0.35 eV trap. Note that the trap E_b is absent; thus, it is related to particular growth details, which is beyond the scope of this study. These DLTS results together with *C–V* profiling clearly show that the trap at 0.75 eV depletes the top GaAs layer and the trap at 0.35 eV depletes the GaAsN layer. Both traps are formed when the GaAsN thickness is increased.

Consider the trap at 0.35 eV that is found in the GaAsN layer. Krispin *et al.*[15] observed a similar trap, which they attributed to an interfacial defect. Polyakov *et al.*[17] also observed a similar trap in MBE-grown GaAsN/GaAs. Therefore, this trap is not related to any particular growth

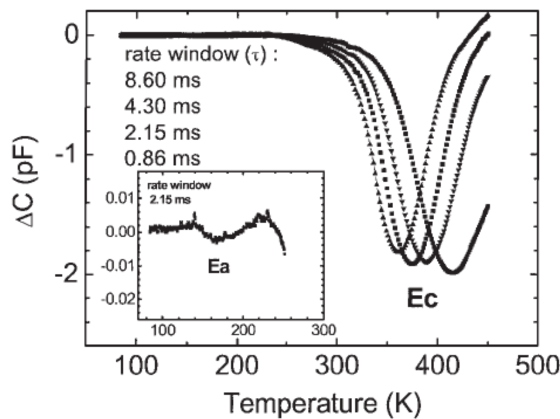

Fig. 6. DLTS spectra of 295-Å sample for top GaAs layer. The predominant trap at about 400 K is the E_c trap and the weak trap is the E_a trap (inset).

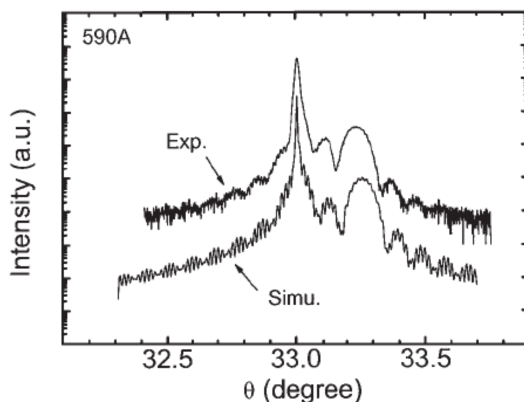

Fig. 7. X-ray spectra along (004) diffraction for 590-Å sample. The peaks at 33.03° and 33.27° correspond to the GaAs and the GaAsN layers, respectively. Also shown are the simulated spectra obtained on the basis of the dynamic theory assuming a coherent strain.

conditions. In terms of its activation energy, this trap is similar to EL6[18] observed in GaAs. The observation that it is formed in thick GaAsN layers grown on GaAs suggests strain relaxation as its origin. However, the XRD patterns show no signs of strain relaxation for the GaAsN layer up to 590 Å. Figure 7 shows the DC-XRD spectra along (004) diffraction for the 590-Å sample. The peaks at 33.03 and 33.27° correspond to the GaAs and GaAsN layers, respectively. Pendellosung interference fringes can be clearly observed, which allow us to accurately determine GaAsN thickness. The presence of these fringes reflects flat GaAsN/GaAs interfaces and suggests a coherent strain.[19] Let us compare the experimental spectra to simulated spectra on the basis of the dynamic theory assuming a coherent strain. During the simulation, the Poisson ratios were taken to be 0.312 and 0.333 for GaAs and GaN, respectively. The lattice constant of GaAsN was obtained from Vegard's law using the lattice constants of 5.653 and 4.526 Å for GaAs and GaN, respectively. As shown in Fig. 7, the experimental spectra agree with the simulated spectra assuming a coherent strain. Therefore, we rule out relaxation as the origin of the trap at 0.35 eV. The exact origin of this trap is not known. As for the trap at 0.75 eV, since it was found mainly in the top GaAs layer, it is not due to N impurity; thus, it is likely to be a GaAs intrinsic defect. Judging from its Ahhrenius plot shown in Fig. 4, it is similar to EL2 observed in GaAs. EL2-like defects were proposed to cause the semi-insulating property in low-temperature (LT)-grown GaAs after annealing.[20] This is consistent with the acceptor-like nature of this trap. The interaction between arsenic antisites (As_{Ga}) and Ga vacancies (V_{Ga}) has been proposed to be EL2-like.[20] Yu *et al.*[21] observed an PL emission at 0.8 eV in LT-grown GaAs and assigned As_i–V_{Ga} for the emission. Irvine and Palmer[22] observed EL2 in InGaAs grown on GaAs and attributed this to an interaction of V_{Ga} with misfit dislocations. Despite different assignments, an As-rich growth condition is commonly accepted for the formation of this trap,[17] suggesting that the growth condition of the top GaAs layer tends to be As-rich. Since the GaAsN layer is not relaxed, the neighboring top GaAs layer is subjected to a considerable compressive strain. Therefore, we speculate that the As-rich growth condition may be related to this compressive strain. This is consistent with the observation of the EL2[22] trap in InGaAs grown on GaAs, in which the InGaAs layer is subjected to compressive strain, and with the absence of the EL2 trap in relaxed GaAs grown on InGaAs,[23] in which the GaAs layer is subjected to tensile strain. The relief of the compressive strain can be realized by removing atoms from their lattice sites,[22] which may favor the formation of V_{Ga} or As_i, resulting in As_{Ga} commonly believed to be a defect related to EL2. The detailed mechanism is not known at this point. Further efforts are required in order to make a more conclusive argument.

4. Conclusion

The properties of GaAsN layers of variously thicknesses grown on GaAs were investigated. When GaAsN thickness is increased, C–V profiling shows carrier depletion in the top GaAs layer and a frequency-dispersion accumulation peak in the GaAsN region. DLTS spectra reveal two traps at 0.35 and 0.75 eV. The trap at 0.75 eV depletes the top GaAs layer and the trap at 0.35 eV depletes the GaAsN layer. The very long emission time for the accumulation peak in the GaAsN region is due to the emptying of electrons from the trap at 0.35 eV. Judging from its Arrhenius plots, the trap at 0.75 eV is EL2-like, suggesting that the growth of the top GaAs layer tends to be As-rich; probably as a result of compressive strain. The formation of these two traps can account for the gradation of I–V characteristics.

Acknowledgment

The authors would like to thank the National Science Council, Taiwan, Republic of China, for financially supporting this research under Contract No. NSC-93-2112-M-009-002.

1) M. Kondow, S. Nakatsuka, T. Kitatani, Y. Yazawa and M. Okai: Electron. Lett. **32** (1996) 2244.
2) S. Sato, Y. Osawa and T. Saitoh: Jpn. J. Appl. Phys. **36** (1997) 2671.
3) L. Bellaiche and A. Zunger: Phys. Rev. B **57** (1998) 4425.
4) S. R. Kurtz, A. A. Alleman, E. D. Jones, J. M. Gee, J. J. Banas and B. E. Hammons: Appl. Phys. Lett. **74** (1999) 729.

5) S. Sakai, Y. Ueta and Y. Teauchi: Jpn. J. Appl. Phys. **32** (1993) 4413.
6) S. H. Wei and A. Zunger: Phys. Rev. Lett. **76** (1996) 664.
7) W. G. Bi and C. W. Tu: Appl. Phys. Lett. **70** (1997) 1608.
8) S. R. Kurtz, A. A. Allerman, E. D. Jones, J. M. Gee, J. J. Banas and B. E. Hammons: Appl. Phys. Lett. **74** (1999) 729.
9) H. P. Xin and C. W. Tu: Appl. Phys. Lett. **72** (1998) 2442.
10) J. Neugerbauer and C. G. Van de Walle: Phys. Rev. B **51** (1995) 10568.
11) Y. Qiu, S. A. Nikishin, H. Temkin, V. A. Elyukin and Yu. A. Kudriavtsev: Appl. Phys. Lett. **70** (1997) 2831.
12) Z. Pan, Y. T. Wang, L. H. Li, H. Wang, Z. Wei, Z. Q. Zhou and Y. W. Lin: J. Appl. Phys. **86** (1999) 5302.
13) E. V. K. Rao, A. Ougazzaden, Y. Le Bellego and M. Juhel: Appl. Phys. Lett. **72** (1998) 1409.
14) S. Francoeur, G. Sivaraman, Y. Qiu, S. Nikishin and H. Temkin: Appl. Phys. Lett. **72** (1998) 1857.
15) P. Krispin, S. G. Spruytte, J. S. Harris and K. H. Ploog: J. Appl. Phys. **88** (2000) 4153.
16) D. Kwon, R. J. Kaplar, S. A. Ringel, A. A. Allerma, S. R. Kurtz and E. D. Jones: Appl. Phys. Lett. **74** (1999) 2830.
17) A. Y. Polyakov, N. B. Smirnov, A. V. Govorkov, A. E. Botchkarev, N. N. Nelson, M. M. E. Fahmi, J. A. Griffin, A. Khan, S. N. Mohammad, D. K. Johnstone, V. T. Bublik, K. D. Chsherbatchev and M. I. Voronova: Solid-State Electron. **46** (2002) 2141.
18) G. M. Martin and A. M. Mitonneau: Electron. Lett. **13** (1977) 191.
19) J. F. Chen, P. Y. Wang, J. S. Wang, N. C. Chen, X. J. Guo and Y. F. Chen: J. Appl. Phys. **87** (2000) 1251.
20) D. C. Look: Thin Solid Films **231** (1993) 61.
21) P. Y. Yu, G. D. Robinson, J. R. Sizelove and C. E. Stutz: Phys. Rev. B **49** (1994) 4689.
22) A. C. Irvine and D. W. Palmer: Phys. Rev. Lett. **68** (1992) 2168.
23) J. F. Chen, P. Y. Wang, J. S. Wang, C. Y. Tsai and N. C. Chen: J. Appl. Phys. **87** (2000) 1369.

VI. SELF EVALUATION

In this proposal, we have investigated the electrical defects in GaAsN layers grown on GaAs. Thick GaAsN layers grown on GaAs are resistive due to the presence of two traps, E_1 at 0.16 eV and E_2 at 0.74 eV. This result indicates that these two traps play a significant role in degrading the electrical quality of a thick GaAsN layer. We also investigated the properties of GaAsN layers of variously thicknesses grown on GaAs. We show that when GaAsN thickness is increased, C-V profiling shows carrier depletion in the top GaAs layer and a frequency-dispersion accumulation peak in the GaAsN region. DLTS spectra reveal two traps at 0.35 and 0.75 eV. The trap at 0.75 eV depletes the top GaAs layer and the trap at 0.35 eV depletes the GaAsN layer. The very long emission time for the accumulation peak in the GaAsN region is due to the emptying of electrons from the trap at 0.35 eV. Judging from its Arrhenius plots, the trap at 0.75 eV is EL2-like, suggesting that the growth of the top GaAs layer tends to be As-rich; probably as a result of compressive strain. The formation of these two traps can account for the gradation of I-V characteristics. We have achieved about 90 % of the works we planed to study in this proposal. This work is very helpful understanding the physical properties of N-related alloys and is important for applications in long-wavelength optoelectronic devices.